

More than Action: The Dorsal Pathway Contributes to the Perception of 3-D Structure

Erez Freud¹, Amanda K. Robinson^{2,3}, and Marlene Behrmann¹

Abstract

■ An evolving view in cognitive neuroscience is that the dorsal visual pathway not only plays a key role in visuomotor behavior but that it also contributes functionally to the recognition of objects. To characterize the nature of the object representations derived by the dorsal pathway, we assessed perceptual performance in the context of the continuous flash suppression paradigm, which suppresses object processing in the ventral pathway while sparing computation in the dorsal pathway. In a series of experiments, prime stimuli, which were rendered imperceptible by the continuous flash suppression, still contributed to perceptual decisions related to the subsequent perceptible target

stimuli. However, the contribution of the prime to perception was contingent on its structural coherence, in that a perceptual advantage was observed only for targets primed by objects with legitimate 3-D structure. Finally, we obtained additional evidence to demonstrate that the processing of the suppressed objects was contingent on the magnocellular, rather than the parvocellular, system, further linking the processing of the suppressed stimuli to the dorsal pathway. Together, these results provide novel evidence that the dorsal pathway does not only support visuomotor control but rather also derives the structural description of 3-D objects and contributes to shape perception. ■

INTRODUCTION

The cortical visual system is almost universally considered to comprise two anatomically and functionally distinct pathways: a ventral occipitotemporal pathway that subserves object perception and a dorsal occipitoparietal pathway that subserves object localization (Ungerleider & Mishkin, 1982) and visually guided action (Goodale & Milner, 1992). Accumulating evidence from both human and nonhuman primate studies, however, challenges this strict binary distinction and suggests that regions in the dorsal pathway also derive object representations and that these representations are computed independently of those in ventral cortex (e.g., Bracci, Daniels, & de Beeck, 2017; Freud, Culham, Plaut, & Behrmann, 2017; Freud, Ganel, et al., 2017; Theys, Romero, van Loon, & Janssen, 2015; Konen & Kastner, 2008; for a review, see Freud, Plaut, & Behrmann, 2016).

However, it remains to be determined whether and in what way these dorsal representations contribute to object perception. Recent evidence for such a contribution comes from a recent TMS study in humans that showed that deactivation of the dorsal pathway impaired the configural processing of faces (Zachariou, Nikas, Safiullah, Gotts, & Ungerleider, 2017). Additional supportive evidence comes from electrophysiology studies in nonhuman primates that showed that reversible inactivation of the

caudal intraparietal sulcus led to impairments in the perceptual 3-D perception of surfaces defined by a single depth cue (stereoscopic; Van Dromme, Premereur, Verhoef, Vanduffel, & Janssen, 2016). Although the findings from such studies reflect engagement of dorsal cortex in perception, they do not specifically examine the role of dorsal cortex in object-based perceptual behaviors per se.

To elucidate the relative contribution of the dorsal pathway to object perception, we adopt an interocular suppression technique, continuous flash suppression (CFS), which renders stimuli imperceptible for up to several seconds (Tsuchiya & Koch, 2005). In this method, a static, low-contrast image is presented to one eye, and a rapidly changing colorful Mondrian pattern is presented to the other eye (see example in Figure 1B). Observers are typically unaware of the static image, which is suppressed by the changing pattern. Both behavioral (Han, Lunghi, & Alais, 2016; Sakuraba, Sakai, Yamanaka, Yokosawa, & Hirayama, 2012; Almeida, Mahon, Nakayama, & Caramazza, 2008; Bahrami, Lavie, & Rees, 2007) and imaging findings (Tettamanti, Conca, Falini, & Perani, 2017; Fang & He, 2005) suggest that the CFS abolishes activation of the ventral pathway but still allows largely intact processing by the dorsal pathway, presumably by the magnocellular system (for a different view, see Ludwig, Kathmann, Sterzer, & Hesselmann, 2015). This arrangement in which dorsal cortex derives representations essentially in the absence of a ventral pathway contribution allows us to evaluate the perceptual role of the dorsal pathway in relative isolation.

¹Carnegie Mellon University, Pittsburgh, PA, ²The University of Sydney, ³Macquarie University, Sydney, Australia

Previous studies have already utilized CFS for a similar purpose and have demonstrated that the dorsal pathway is sensitive to object “toolness” (Tettamanti et al., 2017; Almeida et al., 2008, 2014; Almeida, Mahon, & Caramazza, 2010) and elongation (Almeida et al., 2014; Sakuraba et al., 2012) and that these representations can facilitate perceptual behaviors. Importantly, however, these visual and semantic features (as well as the decisions made by the observers, namely, a tool/animal classification) are tightly linked to visuomotor functions of the dorsal pathway (Tettamanti et al., 2017) and, therefore, do not obviously permit conclusions about the contribution of the dorsal pathway to general object perception.

Previous investigations in human and nonhuman primates have revealed that cortical sites along the dorsal pathway are sensitive to binocular (e.g., Alizadeh, Van Dromme, Verhoef, & Janssen, 2018; Georgieva, Peeters, Kolster, Todd, & Orban, 2009; Durand et al., 2007) and monocular depth cues (Georgieva, Todd, Peeters, & Orban, 2008; Shikata et al., 2001; Taira, Nose, Inoue, & Tsutsui, 2001; for a review, see Orban, 2011). The sensitivity of the dorsal pathway is not limited to depth cues, however, and can reflect the processing of object-based structural description information (Freud, Rosenthal, Ganel, & Avidan, 2015; Theys, Pani, van Loon, Goffin, & Janssen, 2013; Konen & Kastner, 2008; for a review, see Janssen, Verhoef, & Premereur, 2018). However, it is not clear to what extent these dorsal computations contribute to the perception of 3-D, object-based information. To address this, in the current study, we utilized the CFS technique to investigate the contribution of the dorsal pathway to the perception of object-based structural information.

In a series of four experiments, two different sets of novel 3-D stimuli without any clear visuomotor association or salient visual properties (such as elongation) were presented in the context of a relative depth judgment task that did not directly tap visuomotor engagement. On each trial, the target object was preceded by either the same object or a different object, both of which were rendered imperceptible using the CFS (see Figure 1A–B). We hypothesized that the structural description of the CFS-masked prime object is independently computed by the dorsal pathway. We predicted then that, given the spatial nature of the task (i.e., judgment of the relative depth of two dots), the existence of a precomputed structural description that matched the target object would facilitate performance (i.e., a priming effect). However, this facilitation should only be observed when the dorsal pathway could derive a coherent structural description of the object and not when the 3-D information embedded in the prime object was invalid (Experiments 2 and 3).

EXPERIMENT 1

Experiment 1 was set to establish the contribution of the dorsal pathway to the perception of 3-D structural infor-

mation. To this end, target objects were primed by the same or different objects that were rendered imperceptible using the CFS. We measured whether the prime objects modulated the processing of the target objects by comparing the performance observed for “same” and “different” trials.

Methods

Participants

Twenty participants were recruited for this experiment. The data from two participants, who reported that they perceived the masked stimuli during the main experiment, were not analyzed. Data from the remaining 18 participants were analyzed (mean age = 20.3, $SD = 3.61$, 12 female). In this and the subsequent experiments, all participants had normal or corrected-to-normal vision. The experimental procedures complied with the protocol approved by the Carnegie Mellon University Institutional Review Board, and all participants provided informed consent. Some participants received course credit, and others were paid \$10 for their participation.

Stimuli

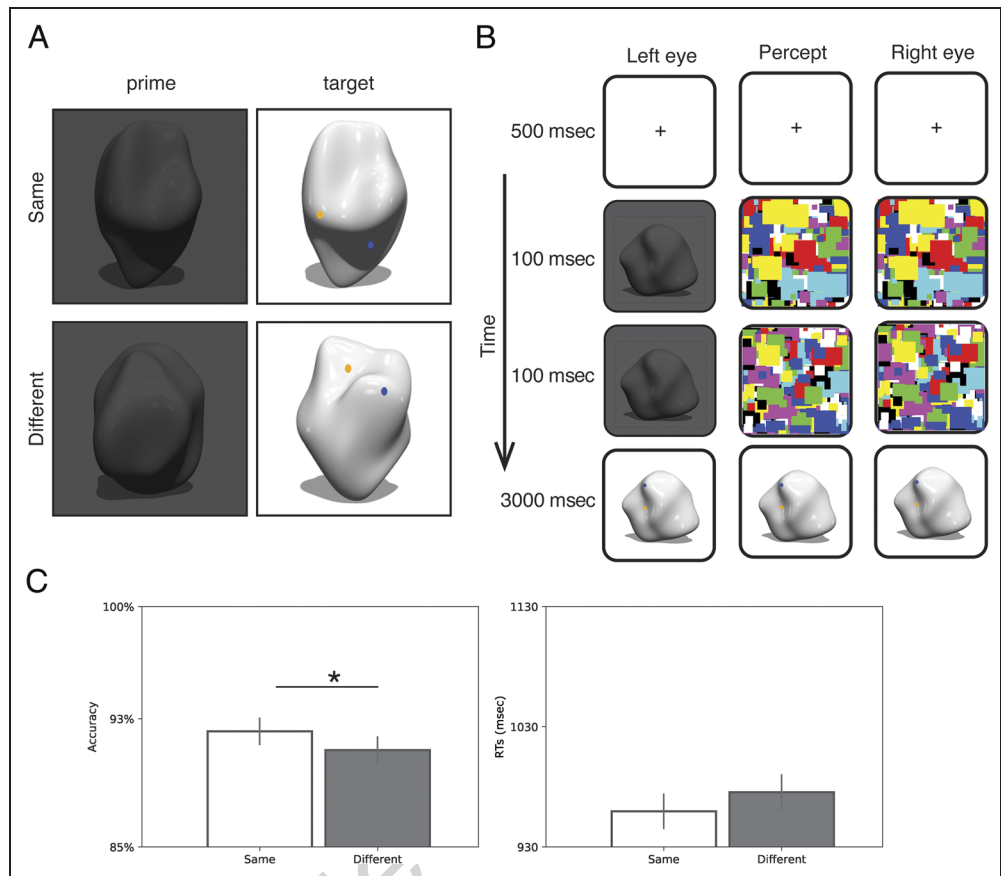
Stimuli were 100 3-D rendered models of novel objects (Figure 1) that had been used in a previous study (Norman, Bartholomew, & Burton, 2008). Depth information was cued by occlusion, texture, and lighting that were superimposed on the original stimuli. For each target object, another image, in which the original object was rotated by 10° on the horizontal plane, was rendered. The rotated objects served as the prime stimuli, and their luminance was reduced to 5% from the original image. The threshold of 5% was set based on a pilot study that demonstrated the effectiveness of the CFS at this level of luminance. Stimuli captured a visual angle of approximately $5.5^\circ \times 5.5^\circ$ (see procedure for a full description of the apparatus), suggesting that the processing of these stimuli relied mainly on central vision mechanisms.

Two dots (blue and yellow) were superimposed on the target stimuli, but not on the masked prime stimuli. The dots were located on different surfaces to encourage the processing of the object as a whole and were positioned such that they were at different depths on the object. In addition, the assignment of the dots was counter-balanced such that, for half of the stimuli, the closer dot was lower in the vertical plane and, for the other half, the closer dot was higher in the vertical plane, and that, on half the trials, the closer dot was blue and, on the other half, it was yellow.

Procedure

The participant’s head was secured in a chin rest. Two mirrors, one at 45° and one at 135° , each reflecting one

Figure 1. Experiment 1: Design and results. (A) Examples of same and different trials. Prime objects were the same (with a 10° offset) or different from the target stimulus. Participants were asked to judge which dot (yellow/blue) was closer to the observer in depth. For presentation purposes, yellow dots are shown here in orange. (B) Sequence of events for an example trial. The right and left columns represent the information presented to each eye separately. The middle column represents the percept of the participant. The dynamic mask suppresses the processing of the information presented to the left eye, and the percept corresponds to the information presented to the right eye. (C) Results: Better accuracy was observed for target images primed by the same than different objects (priming effect). A similar pattern was observed in RT but did not reach statistical significance. In all figures, horizontal lines with an asterisk represent a significant difference between two conditions. Error bars are the confidence interval (95%) of the priming effect.



of two monitors, were arranged in front of the participant. The total viewing distance was 63.5 cm, which resulted from the distance from the chin rest to the center of the mirror (8 cm) and from the distance from the center of the mirror to the monitor on the same side (55.5 cm). Two black dividers were attached to the chin rest, blocking the participant's direct view of the monitors, with the result that the display was only visible in the mirror. Stimuli were presented using Matlab Psychtoolbox (Brainard, 1997). At the beginning of the experiment, participants completed a calibration procedure to ensure that the images from the two screens were fused. Two fixation crosses were presented, one on each monitor, and the participants used the keyboard to move the fixation crosses until the two crosses reached a position in which they were perceived as a single, fused cross.

A single trial started with a fixation cross (500 msec) presented to both eyes, followed by a dynamic (10 Hz) random colorful (Mondrian) pattern that was presented to the right eye, whereas a static, low contrast (5% of the original image, a threshold that was found to be efficient in a pilot experiment) stimulus was presented to the left eye (200 msec) and served as the prime image (see Figure 1). The target object was then presented to both eyes. Participants were required to judge which of the

two dots was located closer in depth. The target object remained on the screen until the participant responded by pressing the designated keyboard keys ("f" for blue and "g" for yellow) or for a maximum period of 3 sec.

Experiment 1 included a total of 200 trials in which the target object was primed by the same object that differed from it by a 10° viewpoint offset on the horizontal plane ("same") or by a different object ("different"). This ensured that the primes and targets within a same trial contained the same object but were not identical images. The colored dots were never superimposed on the prime objects. Each target object was presented twice during the experiment (once following the same prime and once following a different prime).

Control Experiment

After completing the main experiment above, participants were asked whether they perceived the prime objects. Participants who perceived the prime stimuli were excluded from the analysis ($N = 2$). All other participants completed an additional control detection task to evaluate the effectiveness of the CFS procedure. The experiment included a total of 100 trials. Similar to the main experiment, the dynamic mask was presented for

200 msec to the right eye. At the same time, a novel object, similar to the ones used in the main experiment, was presented to the left eye on 50% of the trials, whereas an empty gray square was presented on the remaining trials. Participants were told that a stimulus might be presented at the same time as the dynamic mask, and they were asked to report whether an object was presented and responded by pressing the designated keyboard keys (“f”—no object, “k”—object).

Results

Accuracy of depth judgment was high (91.6%, $SD = 4\%$), and better performance was observed for target images that were primed by the same object (92.2%) compared with a different object (91.0%), $F(1, 17) = 4.521, p < .05, \eta_p^2 = .21$. A similar pattern was observed for response speed, with shorter RTs for the same trials, although it did not reach statistical significance, $F(1, 17) = 2.62, p = .12, \eta_p^2 = .13$ (Figure 1C).

A follow-up control experiment (see Methods for details) ensured the effectiveness of the CFS procedure by showing that the same participants performed poorly on a masked object detection task (mean accuracy = 51.5%, $SD = 2.7\%$). Performance was significantly above chance level, $t(17) = 2.28, p < .05$, but clearly participants were largely unaware of the masked object in this paradigm. Moreover, for each participant, a z test for a single proportion validated that the performance was not different from chance ($p > .5$, FDR corrected for multiple comparisons).

The results of Experiment 1 are straightforward. Prime objects, suppressed by the dynamic mask, facilitated performance in the depth decision task. Importantly, the retinal image of the prime and target was different for both the same and the different trials, indicating that the representation of the prime object was not limited to 2-D attributes but, rather, was related to the shared 3-D structure of the prime and target object. A control experiment confirmed the effectiveness of the mask in suppressing the detection of the prime stimulus.

EXPERIMENT 2

Experiment 1 provided novel evidence that stimuli, suppressed by the CFS and processed primarily by the dorsal pathway, can facilitate subsequent perceptual decisions related to object 3-D structure. These representations were derived for objects that did not convey clear visuo-motor associations. Moreover, the prime and target objects on “same” trials were presented from a different viewpoint, reinforcing the notion that the 3-D structure of the prime object facilitated the depth decision.

Although we have suggested that the superior performance observed in Experiment 1 for the same prime–target pairs over different prime–target pairs was a function of dorsal cortex facilitation, there is an alternative account

of the findings. This alternative view suggests that the priming effect is contingent on the visual similarity between the prime and the target stimuli (which are still more similar to each other than is true for the different trials) and not on the representation of 3-D information.

Experiment 2 was designed to adjudicate between these two explanations. If the dorsal pathway representations are anchored to the 3-D description of the object (and not to visual similarity at the 2-D level), we would not expect to observe priming when stimuli do not have coherent 3-D structure, even when the prime and the target object are visually similar.

Participants were presented with displays of target objects, which were primed by 3-D spatially possible or impossible objects. Importantly, the images of impossible objects were visually highly similar to the possible objects but violated the laws of 3-D spatial organization and therefore could not be reconstructed in real 3-D space (e.g., Freud, Ganel, et al., 2017; Freud, Rosenthal, et al., 2015). As in Experiment 1, the task was to classify which of two dots, located on an object, was closer to the observer in depth. The priming effect was estimated by the comparison between same and different trials, separately for each object type.

Methods

Participants

Twenty-eight participants were recruited for this experiment. The data from two participants were not analyzed, as they reported that they perceived the masked stimuli during the main experiment. The data of one additional participant were excluded as their performance for one or more of the types was poor (below 70% compared with group mean accuracy ~90%). Data from the remaining 25 participants were analyzed (mean age = 19.5, $SD = 1.91$, 13 female).

Stimuli

Stimuli were 71 grayscale line drawings of impossible objects, all of which have been used in previous studies (Freud & Behrmann, 2017; Freud, Ganel, et al., 2017; Freud, Ganel, & Avidan, 2015). For each impossible object, a matched possible object was derived by minimally altering visual features to modify the object’s global structure from impossible to possible. There were no obvious differences in image statistics of the possible and impossible images as demonstrated by comparisons showing equivalence in the overall number of pixels (37,323 vs. 37,365 for possible vs. impossible objects, respectively) and the number of pixels that defined the object’s edges (3738 vs. 3730 for possible vs. impossible objects, respectively). Finally, the average pixel-wise correlation between matched possible and impossible objects was $r = .96$, whereas the average correlation of

the nonmatched objects was $r = .22$, further reflecting the high visual similarity between the matched objects.

As in Experiment 1, the luminance of the prime stimuli was reduced to 5% from the original value, and one green dot and one red dot were superimposed on the target objects. The assignment of the dots was done based on the following logic. First, the dots were located on different surfaces to encourage the processing of the object as a whole. Second, the dots were located in the same position for the possible and matched impossible target objects to maximize the similarity between object categories. Third, the dots were not placed on the junctions that induced object impossibility, thus precluding an objective “correct” decision in the depth task for the two object categories. Finally, the assignment of the dots was counterbalanced across stimuli such that, for half of the stimuli, the closer dot was lower in the vertical plane and, for the other half, the closer dot was higher in the vertical plane and that, on half the trials, the closer dot was red and, on the other half, it was green.

The experiment included a total of 212 trials in which the target object was either possible or impossible. To avoid a between-type priming effect, each participant was exposed to only one version of a particular stimulus (possible or impossible; counterbalanced across participants). The prime image was either identical to the target object (same), a different object from the same category (different) or a gray square (no object). The “no-object” condition was not included in the analysis because, in retrospect, it was not comparable to the same or different trials both of which contained considerable visual information.

Control Experiments

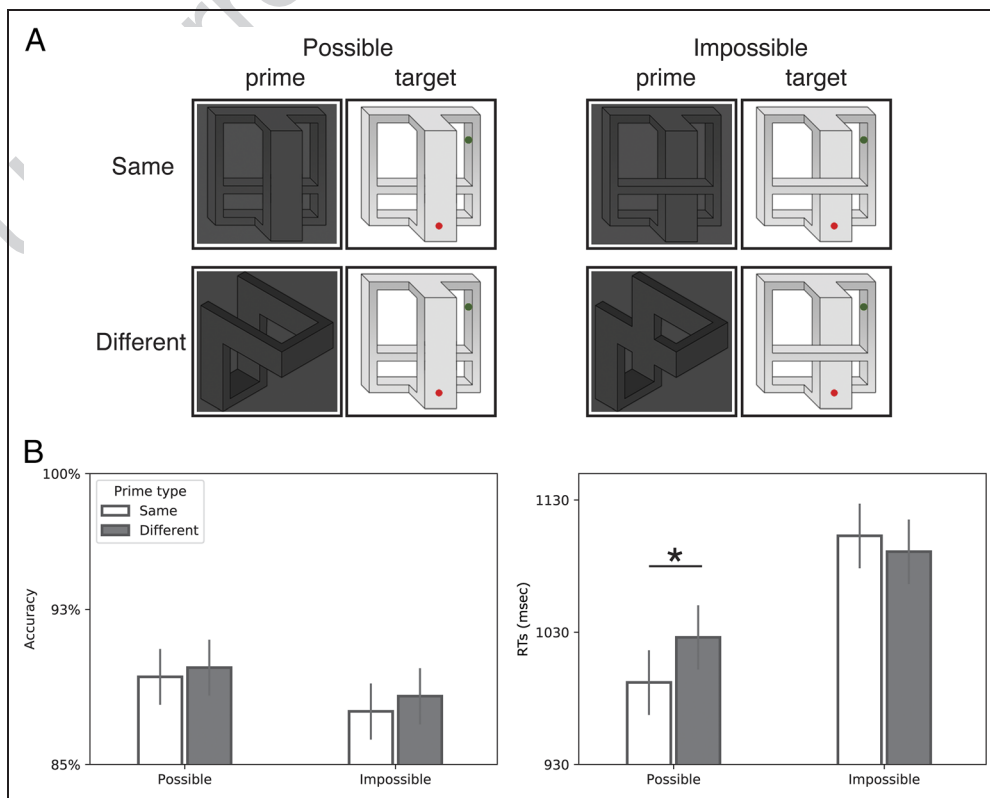
Following the main experiment, participants were asked whether they perceived the prime objects. Participants who perceived the prime stimuli were excluded from further analysis. Participants completed two control experiments. The detection task (see Experiment 1 for details) included a total of 80 trials, in which participants were asked to detect whether an object (possible/impossible) was present or not. To confirm further the effect of the mask, an additional classification task, with a total of 140 trials, was employed. During this experiment, a dynamic mask was presented for 200 msec to the right eye, and an object was presented to the left eye. The objects (possible and impossible) were either intact or scrambled, and participants were asked to classify the status of the object (intact/scrambled).

Results

Accuracy in the depth decision task was high (mean = 88.9%, $SD = 4\%$), and no priming effect nor interaction between object type and priming type was found, $F_s(1, 24) < 1$. Analysis of the RT, however, showed that, for possible target objects, a priming effect was observed, with faster RTs for trials primed by the same object, compared with the different object. In contrast, for impossible objects, there was no evidence of a priming effect (Figure 2B).

A repeated-measures ANOVA on the RT data, with object type (possible, impossible) and priming condition

Figure 2. Experiment 2: Design and results. (A) Examples of same and different trials. Prime objects were similar or different from the target stimuli that were either structurally possible or impossible. Participants were asked to judge which dot (green/red) was closer to them in depth. (B) Results: RT analysis revealed a priming effect for possible but not for impossible objects that lacked a coherent 3-D structural description.



(same, different object) as independent, within-subject variables revealed a robust main effect of object type, $F(1, 24) = 22.63, \eta_p^2 = .48, p < .001$, such that participants were faster to respond to possible objects relative to impossible objects, reflecting the sensitivity of the visual system to structural impossibility (Freud & Behrmann, 2017; Freud, Ganel, et al., 2017; Freud, Rosenthal, et al., 2015). More importantly, an interaction between Object type \times Priming condition was found, $F(1, 24) = 4.28, \eta_p^2 = .15, p < .05$. Simple comparisons confirmed that, for possible objects, a priming effect was observed with 37 msec faster RT for trials primed by the same object compared with trials primed by a different object, $F(1, 24) = 4.54, p < .05$. Interestingly, for impossible objects, no such priming was observed, $F(1, 24) < 1$, suggesting that if the prime object violates legitimate 3-D structure, a 3-D representation cannot be derived under CFS (and thus has no subsequent effect on behavior).

Note that, in contrast to Experiment 1 (and to Experiment 4, see below), the priming effect in this experiment (as well as in Experiment 3, see below) was evident in terms of RT and not in terms of accuracy. For completeness, we have presented both measures for every experiment. That the key effect manifests in different dependent measures for different experiments might be related to the structural possibility of the targets, namely in Experiments 2 and 3, but not in Experiments 1 and 4, impossible targets were included. The structural incoherence of the impossible objects might have increased the perceptual uncertainty of observers, even in relation to the possible objects, and consequently modulated the decision-making process applied by the observers. In other words, the presence of an impossible object serves as a context effect that alters the observer's decision-making even for the possible objects (much like when nonwords are included with words in a list, lexical decision even of the legitimate words is adversely affected; Lupker & Pexman, 2010). We directly examined this uncertainty hypothesis by comparing the performance observed for Experiments 2 and 4. The description of this statistical quantification is included in the results section of Experiment 4.

Two follow-up experiments with the same participants (see Methods for details) ensured the effectiveness of the CFS procedure. The first control experiment showed that participants were unable to detect the presence of a masked object even when they were informed that objects were present on half of the trials (mean accuracy = 50.8%, $SD = 3\%$; difference from chance level $t(24) = 1.28, p > .2$). The second control experiment showed that participants were unable to classify whether the masked object was intact or scrambled (mean accuracy = 52%, $SD = 5\%$; difference from chance level $t(21) = 1.71, p > .05$). As was done in Experiment 1, for each participant a z test for a single proportion validated that the performance was not different from chance (all $ps > .1$, corrected for multiple comparisons).

EXPERIMENT 3

The results of Experiment 2 replicate and extend the results of Experiment 1. First, we showed that imperceptible prime objects, presumably processed by the dorsal pathway, can support 3-D perceptual classification, and this held across the two sets of objects that differed substantially in their visual and spatial properties, those from Experiment 1 and those from Experiment 2. Second, the priming effect was observed only for possible but not for impossible 3-D objects, indicating that the priming effect, presumably mediated by dorsal computations, was contingent of the processing of legitimate 3-D information, rather than on visual similarity per se.

In Experiment 2, the prime and the target could be possible and impossible; hence, the facilitation for the possible but not impossible cases might have arisen because of the status of the prime or because of the status of the target. To adjudicate between these two alternatives, in Experiment 3, the target objects were always impossible and were primed by one of the following objects: the same impossible object (same), a visually similar, possible version of the target object (matched possible), or a different impossible object (different; Figure 3A). If the lack of the priming effect for impossible objects in Experiment 2 reflects the difficulty processing impossible prime stimuli, the counterintuitive prediction is that no priming effect would be observed for trials even when the target is primed by the same impossible object. In contrast, a visually similar (but not identical) possible prime will enable the dorsal pathway to derive a 3-D representation, which, in turn, would facilitate the perceptual decision, even when the target object is impossible.

Methods

Participants

Twenty-six participants were recruited for this study. The data from two participants were not analyzed since they reported that they perceived the masked stimuli during the main experiment. The data from the remaining 24 participants were analyzed (mean age = 22.3, $SD = 4$, 14 female).

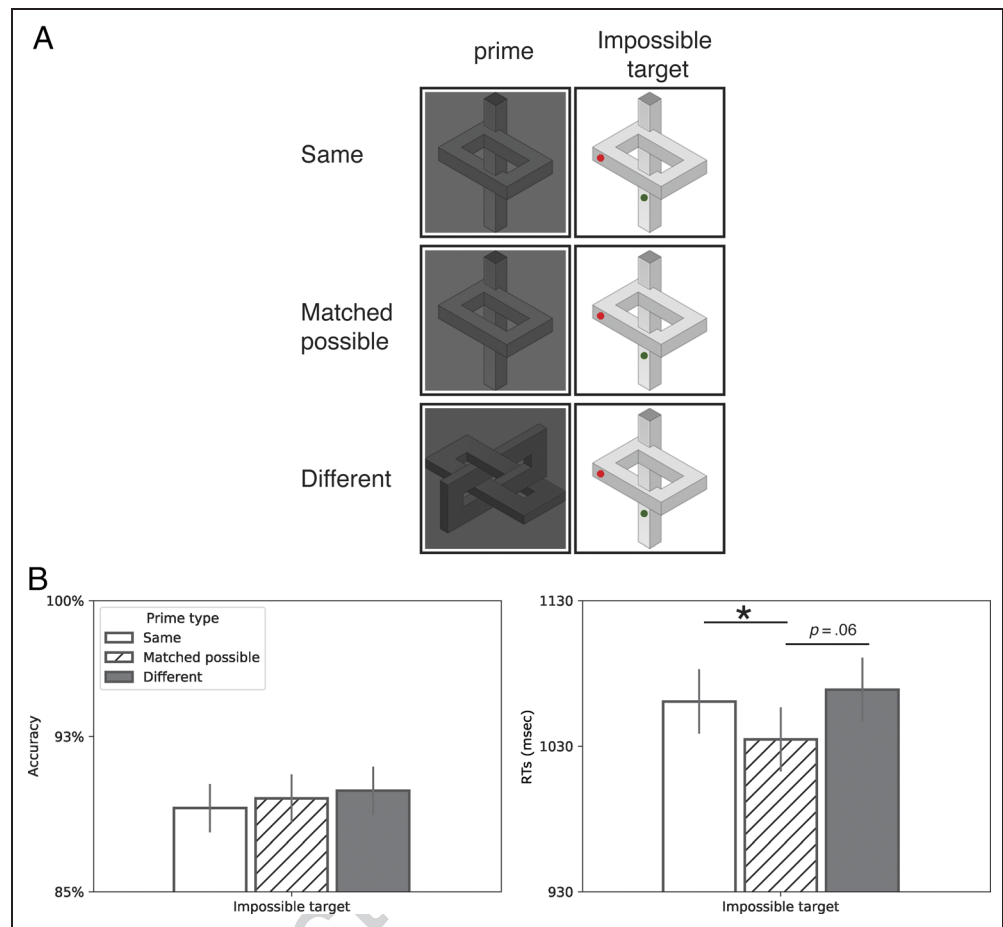
Stimuli

The stimuli were identical to the stimuli used in Experiment 2. However, in Experiment 3, only impossible objects served as target objects.

Procedure

The procedure was similar to that used in Experiment 2, except for the following changes. The experiment included a total of 212 trials in which the target object was always impossible. The trials were drawn

Figure 3. Experiment 3: Design and results. (A) The target object was always impossible and was primed by the same impossible object, a visually similar, but possible, version of the object or a different impossible object. (B) Results: A priming effect was found when the target objects were primed by a matched (visually similar, but not identical) possible version of the same object and not when the object was primed by an identical impossible or a different object.



equiprobably from three conditions: when the prime image was either identical to the target (same), the possible version of the target (matched possible), or a different impossible object (different). Each target object was primed by each of the three conditions.

Control Experiments

Similar to Experiment 2, two control experiments were employed following the main experiment. Participants performed a detection task (a total of 76 trials) and a categorization task (a total of 140 trials) for objects suppressed by CFS. See Experiment 2 Methods for details.

Results

The results of Experiment 3 are presented in Figure 3B. Accuracy of depth decision was high (89.7%), with no priming effects, $F(1, 46) < 1.2, p > .25$. Interestingly, trials primed by a matched possible object had shorter RTs relatively to trials primed by an impossible object, even when the impossible prime object was identical to the target object. Planned comparisons validated that matched possible primes led to faster RTs than the same

impossible objects and different impossible primes, $F(1, 46) = 5.28, p < .05$. In contrast, no difference was observed between same-impossible and different-impossible trials ($F < 1$), replicating the lack of priming for impossible targets primed by an impossible object. Thus, Experiment 3 provides converging evidence for the functional role of the dorsal pathway in perceptual decisions related to 3-D structure and is compatible with the notion that these dorsal representations are sensitive to the legality of object geometry.

Similar to Experiment 2, two follow-up experiments ensured the effectiveness of the CFS procedure by showing that participants were at chance in detecting the presence of a masked object (mean accuracy = 50%, $SD = 6\%$; difference from chance level $t(23) < 1$) and were also at chance in classifying whether the masked object was intact or scrambled (mean accuracy = 51%, $SD = 6\%$; difference from chance level $t(23) = 1.04, p > .05$). As was done in the first two experiments, for each participant a z test for a single proportion validated that the performance was not different from chance. One participant's data deviated from chance in one of the two control experiments. Thus, the main analysis was conducted after excluding this participant, and the results reported above remained the same.

EXPERIMENT 4

Experiments 1–3 show that, notwithstanding the absence of overt perception of the prime stimuli presented in a CFS paradigm, stimuli with coherent but not incoherent 3-D structure still modulated perceptual performance. The main hypothesis is that the processing of the suppressed (prime) image is mediated by dorsal pathway computations, because the CFS perturbs object processing primarily in the ventral visual pathway and, to a lesser degree (if at all), in the dorsal visual pathway. This hypothesis is supported by imaging (Tettamanti et al., 2017; Fang & He, 2005) and behavioral evidence (Han et al., 2016), although the neural underpinnings of the CFS phenomena still remain debatable (Moors, Hesselmann, Wagemans, & van Ee, 2017; Ludwig & Hesselmann, 2015; Ludwig et al., 2015). Experiment 4 was designed specifically to explore the neural underpinnings of the priming effects observed in Experiments 1–3.

To this end, we utilized a psychophysics technique that biases the processing of a visual stimulus to the magnocellular system or, alternatively, to the parvocellular system. Notably, whereas the ventral pathway gets a significant amount of input from the parvocellular system, the dorsal pathway receives most of its input from the magnocellular system (Merigan & Maunsell, 1993) and the koniocellular (K) system (Almeida, Fintzi, & Mahon, 2013). Although this separation is relative, rather than binary (Nassi, Lyon, & Callaway, 2006; Ferrera, Nealey, & Maunsell, 1994), previous studies have utilized this characteristic to investigate the differential nature of representations along the two pathways (Kristensen, Garcea, Mahon, & Almeida, 2016; Almeida et al., 2013; Mahon, Kumar, & Almeida, 2013; Thomas, Kveraga, Huberle, Karnath, & Bar, 2012). If the priming effect observed in Experiments 1–3 relies on dorsal and not ventral representations, as we have surmised, only a magnocellular-biased prime, which facilitates dorsal pathway processing, should elicit a priming effect. In contrast, the parvocellular-biased prime, which biases the processing to the ventral pathway, should not elicit a priming effect.

Methods

Participants

Forty-five participants completed this experiment. The data of two participants were excluded because their accuracy in the main task for one or more of the categories was below 70% (mean accuracy \sim 90%). The data from the 43 remaining participants (Experiment 4, mean age = 21.1, SD = 3.3, 30 female) were analyzed.

Stimuli

Both prime and target stimuli were only possible objects, and these were taken from Experiments 2 and 3. Two types of stimuli were used as the prime. Grayscale, low-

contrast (luminance of 5%) stimuli were aimed at stimulating the magnocellular system, and the same stimuli, but now colored red and green, were aimed at biasing the processing to the parvocellular system. Note that previous experiments (Thomas et al., 2012) generated isoluminant stimuli that were adjusted individually for each subject. In the present experiment, we could not replicate this titration procedure because (a) the stimuli were presented simultaneously with a colorful mask that likely alters the sensitivity and (b) the generation of isoluminant stimuli requires individual calibration. Employing this calibration procedure could alert the participants to the presence of such stimuli, and this, in turn, might impair the effectiveness of the CFS procedure.

In contrast with Experiments 2 and 3, the dots for the depth detection task were colored blue and yellow to avoid plausible interaction with the parvocellular-biased prime stimuli.

Procedure

Experiment 4 included a total of 140 trials in which the target object was always possible. The prime image was either identical to target object (same) or a different object (different). Half of the prime images were colored red and green to activate specifically the parvocellular system. The other half of the prime images were grayscale (similar to Experiments 1–3) and stimulated the magnocellular system. Each stimulus was presented twice throughout the experiment and was primed by either parvocellular-biased or magnocellular-biased images (counterbalanced across participants).

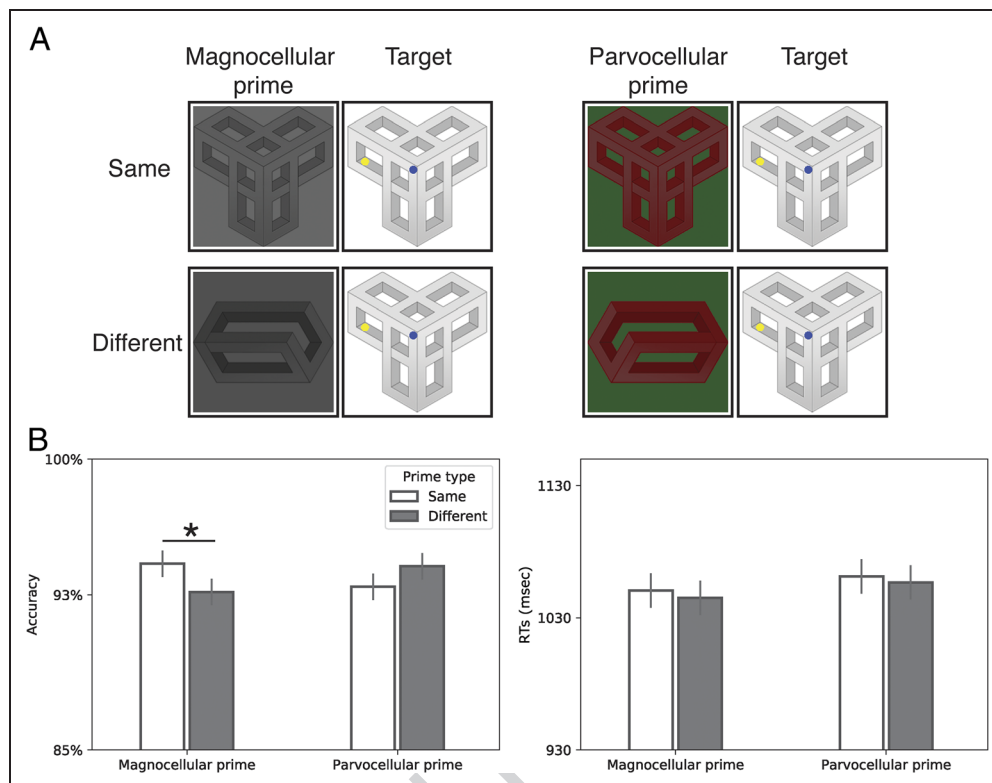
Control Experiment

In the classification control task (140 trials), participants were asked to report whether the suppressed stimulus was intact or scrambled (see Experiment 2 Method). Importantly, the experiment included parvocellular-biased and magnocellular-biased stimuli to evaluate whether the mask was equally efficient for the different prime types.

Results

Participants were presented with displays of structurally possible objects, which were preceded by a same or a different possible prime object that was either parvocellular-biased (defined by color) or magnocellular-biased (achromatic). As in Experiments 1–3, the task was to classify which of two dots, located on a possible target object, was closer to the observer in depth. As before, the prime objects were presented to the left eye and were suppressed by the presentation of a dynamic random noise (10 Hz) to the right eye (Figure 4A).

Figure 4. Experiment 4: Design and results. (A) Examples of the prime and targets for same and different trials. Prime objects were similar or different from the target stimulus and were either grayscale or red–green images to bias the processing to the magnocellular or parvocellular systems, respectively. Participants were asked to judge which dot (yellow/blue) was closer to them in depth. (B) Results: A priming effect was found only for the magnocellular-biased prime images and not for the parvocellular-biased prime images.



Accuracy in the depth detection task was high (93.9%). A repeated-measures ANOVA with prime type (parvocellular-biased/magnocellular-biased) and trial type (same/different) revealed a significant two-way interaction, $F(1, 42) = 5.14$, $\eta_p^2 = .11$, $p < .05$. Simple comparisons showed that, for magnocellular-biased primes (i.e., grayscale), higher accuracy was observed for same trials (93.3%) than for different trials (92.2%), $F(1, 42) = 3.98$, $p = .05$. On the other hand, no difference was observed for the parvocellular (i.e., red–green) stimuli, $F(1, 42) = 2.07$, $p > .15$. Notably, the existence of a priming effect in terms of accuracy is consistent with the uncertainty hypothesis (see Experiment 2 and below), because only possible objects were included in this experiment.

The analysis of the RTs did not reveal main effects nor an interaction effect ($F_s < 1$). These findings suggest that the priming effects observed in Experiments 1–4 were mediated by the magnocellular system, and as such, provide additional support for the notion that the dorsal, rather than the ventral, pathway supported the CFS priming effects.

As described above, the CFS priming effect was manifested in terms of accuracy (similar to Experiment 1), but not in terms of RT (as was found in Experiments 2 and 3). The main hypothesis was that the discrepancy across the dependent measures might be explained by the uncertainty elicited by the inclusion of impossible objects. To examine this hypothesis, we compared the accuracy and RT observed for the possible objects in Experiments 2 and 4. Importantly, in both experiments the possible ob-

jects were similar, but in Experiment 2 these possible objects occurred in the same study with impossible objects, whereas in Experiment 4 only possible objects were ever presented. We focused our analysis only on the different trials to exclude the effect of the prime objects. In accordance with the uncertainty hypothesis, a robust effect of experiment was found, with better accuracy for Experiment 4, in which only possible objects were presented, $F(1, 66) = 11.96$, $p < .01$, $\eta_p^2 = .15$. This finding suggests that, when possible, objects alone were shown accuracy served as a reliable, dependent measure to estimate the effect of the CFS prime objects. On the other hand, when impossible objects appeared among the stimuli and uncertainty in decision-making arose, priming effects were more reliably estimated by RT.

Finally, the classification control experiment validated the effectiveness of the mask for the two prime types. Classification accuracy was 50.3% for the magnocellular-biased images and 50.4% for the parvocellular-biased images. Paired-sample t test verified that there was no difference between the two image categories, $t(42) < 1$, and one-sample t tests validated that classification accuracy for the two categories were not different from chance ($t_s < 1$). Both magnocellular- and parvocellular-biased images were therefore adequately masked using CFS, yet only the magnocellular-biased primes conveyed an advantage in the main depth task. Similar to Experiments 1–3, for each participant a z test for a single proportion validated that the performance was not different from chance (all $p_s > .25$, corrected for multiple comparisons).

GENERAL DISCUSSION

Accumulating evidence from investigations using human imaging (e.g., Bracci et al., 2017; Freud, Culham, et al., 2017; Zachariou, Klatzky, & Behrmann, 2014; Konen & Kastner, 2008) and from studies with neuropsychological patients (Freud, Ganel, et al., 2017) and nonhuman primates (e.g., Van Dromme et al., 2016; Theys et al., 2015; Durand et al., 2007; Denys et al., 2004) have demonstrated that the dorsal visual pathway derives representations from objects in the environment. This is true even under conditions that are not related to visuomotor control of the objects, and moreover, these representations are dissociable from ventral object representations. These findings challenge the binary distinction between the functions supported by the two visual pathways. An open question, however, is whether representations derived by the dorsal pathway contribute functionally to perceptual, object-based decisions. To address this, in four experiments, we exploited the CFS paradigm, which suppresses the ventral pathway function to demonstrate that the largely isolated dorsal pathway can contribute to perceptual decisions, at least to those related to object 3-D structure.

Experiment 1 demonstrated that novel objects, which were rendered imperceptible by the CFS and were primarily processed by the dorsal pathway, can facilitate object-based decisions related to the object 3-D structure, even when the prime and the target object were presented from different viewpoints. Experiment 2 demonstrated that the CFS priming effect was evident only for possible, but not for impossible, objects, suggesting that the dorsal pathway is tuned to 3-D object description, but only if the visual input is geometrically legal. Experiment 3 elaborated these findings and ensured that the lack of a priming effect for impossible objects could not be attributed to the nature of the target object but rather to the structural incoherence of the prime object—this result further reflects the sensitivity of the dorsal pathway to the legality of the geometrical information. In addition, this experiment converged with the conclusion of Experiment 1 and showed that the priming effect was not contingent on low-level feature similarities between the prime and target. Finally, Experiment 4 utilized an image-based manipulation to uncover the neural substrate of the CFS priming effect and showed that the priming effect relied on the magnocellular system that largely projects to the dorsal pathway and not on the parvocellular system that largely projects to the ventral pathway.

The CFS paradigm has been used previously to demonstrate the contribution of the dorsal pathway to the representations of specific visual categories (i.e., man-made tools), presumably based on the visuomotor associations conveyed by these objects (Almeida et al., 2008, 2010). For example, one recent imaging study, which supports this interpretation, found that images of tools, masked by CFS, activated both the posterior parietal cor-

tex and the ventral premotor cortex (Tettamanti et al., 2017). Consistent with this, several studies have documented that a nontool object can prime perceptual decisions, provided that the nontools are elongated and offer affordances related to action (Almeida et al., 2014; Sakuraba et al., 2012). Because these priming effects likely rely on visuomotor associations and affordances, one cannot make inferences about a functional contribution of the dorsal pathway to perception independent of the contribution to action. Here, by using two different sets of novel objects (i.e., possible and impossible objects, and the 3-D stimuli used by Norman et al., 2008), we show that the dorsal pathway contributes to perceptual decisions, independent of obvious visuomotor associations. Future research can elaborate this line of research and investigate whether other types of spatial perceptual decisions (e.g., geometrical organization of 2-D images) are also supported by computations carried out by the dorsal visual pathway.

The Nature of Object Representations in the Dorsal Pathway

The current study builds upon a growing body of literature that has characterized the nature of the visual representations computed by the dorsal pathway. These investigations revealed that the dorsal pathway can extract shape information independent of the ventral pathway (Kristensen et al., 2016; Almeida et al., 2013). These dorsal representations were sensitive to shape information (Freud, Culham, et al., 2017; Konen & Kastner, 2008) and, in particular, to 3-D information (for reviews, see Freud et al., 2016; Theys et al., 2015; Orban, 2011).

The findings from the present investigation elucidate further the nature of the representation derived by the dorsal pathway and, more importantly, link those representations to perceptual (rather than visuomotor) behaviors. In all four experiments reported here, the prime stimuli, which were presumably processed primarily by the dorsal pathway, contributed to decisions related to the 3-D structure of the targets. Based on these findings, we have proposed that the dorsal pathway computes the 3-D structural description of the prime stimuli and that this description contributes to perceptual processes related to the 3-D structure of the target object. This conclusion is compatible with a neuropsychological investigation in which patients with visual agnosia and profound perceptual impairments resulting from ventral lesions nevertheless revealed sensitivity to 3-D structural information (Freud, Ganel, et al., 2017).

Importantly, previous investigations also suggest that the dorsal pathway representations are not monolithic and, instead, can vary as function of location and task. For example, sensitivity to shape information, as well as correlation with perceptual behaviors, decreases along the posterior–anterior axis of the parietal cortex (Freud, Culham, et al., 2017), and the anterior parts of the dorsal

pathway (e.g., anterior IPS) appears to derive representations based on a combination of visual and motor cues (Freud et al., 2018; Fabbri, Stubbs, Cusack, & Culham, 2016; for electrophysiological results, see Murata, Gallese, Luppino, Kaseda, & Sakata, 2000). Finally, even within the same cortical regions, dorsal pathway representations are susceptible to task demands (Bracci et al., 2017; Jeong & Xu, 2016). Although the present investigation does not allow us to pinpoint the dorsal site/s that might have contributed to the priming effects, based on previous results, the posterior portion of the IPS is a suitable candidate region for these computations.

Finally, although the results of the four experiments confirm a functional role of the dorsal pathway in 3-D object perception, it remains to be determined whether the dorsal representations only contribute to perception or are, in fact, necessary for intact perception. Despite initial evidence that supports the latter interpretation (Zachariou et al., 2017; Van Dromme et al., 2016), future research with patients and animal models should address this important question further and characterize the functional and possibly necessary role of the dorsal visual pathway in object perception.

Conclusions

To conclude, this study exploited the known properties of the CFS paradigm to investigate the functional contribution of the dorsal visual pathway to object perception. In a series of experiments, we demonstrated that stimuli suppressed by CFS nevertheless supported perceptual classification that was contingent on the 3-D structure of the object. Together, these results provide novel evidence for a contribution of the dorsal pathway to 3-D object perception and suggest that the dorsal pathway not only derives geometric description of objects in the service of action but in the service of perception, as well.

Acknowledgments

This study was supported by the Yad-Hanadiv Postdoctoral Fellowship to E. F., by the Israel Science Foundation (Grant 65/15) to E. F., and by a grant from the National Science Foundation (BCS0923763 PI: Behrmann). The authors thank J. Farley Norman for sharing the Norman et al. stimuli with us and Isabel Bleimeister and Alan Lu for their contribution to data collection.

Reprint requests should be sent to Erez Freud, Department of Psychology and the Center of Neural Basis of Cognition, Carnegie Mellon University, Baker Hall, 5000 Forbes Ave., Pittsburgh, PA, or via e-mail: erezfreud@gmail.com.

REFERENCES

Alizadeh, A.-M., Van Dromme, I., Verhoef, B.-E., & Janssen, P. (2018). Caudal intraparietal sulcus and three-dimensional vision: A combined functional magnetic resonance imaging and single-cell study. *Neuroimage*, *166*, 46–59.

- Almeida, J., Fintzi, A. R., & Mahon, B. Z. (2013). Tool manipulation knowledge is retrieved by way of the ventral visual object processing pathway. *Cortex*, *49*, 2334–2344.
- Almeida, J., Mahon, B. Z., & Caramazza, A. (2010). The role of the dorsal visual processing stream in tool identification. *Psychological Science*, *21*, 772–778.
- Almeida, J., Mahon, B. Z., Nakayama, K., & Caramazza, A. (2008). Unconscious processing dissociates along categorical lines. *Proceedings of the National Academy of Sciences, U.S.A.*, *105*, 15214–15218.
- Almeida, J., Mahon, B. Z., Zapater-Rabero, V., Dziuba, A., Cabaço, T., Marques, J. F., et al. (2014). Grasping with the eyes: The role of elongation in visual recognition of manipulable objects. *Cognitive, Affective, & Behavioral Neuroscience*, *14*, 319–335.
- Bahrami, B., Lavie, N., & Rees, G. (2007). Attentional load modulates responses of human primary visual cortex to invisible stimuli. *Current Biology*, *17*, 509–513.
- Bracci, S., Daniels, N., & de Bock, H. O. (2017). Task context overrules object- and category-related representational content in the human parietal cortex. *Cerebral Cortex*, *27*, 310–321.
- Brainard, D. H. (1997). The psychophysics toolbox. *Spatial Vision*, *10*, 433–436.
- Denys, K., Vanduffel, W., Fize, D., Nelissen, K., Peuskens, H., Van Essen, D., et al. (2004). The processing of visual shape in the cerebral cortex of human and nonhuman primates: A functional magnetic resonance imaging study. *Journal of Neuroscience*, *24*, 2551–2565.
- Durand, J.-B., Nelissen, K., Joly, O., Wardak, C., Todd, J. T., Norman, J. F., et al. (2007). Anterior regions of monkey parietal cortex process visual 3D shape. *Neuron*, *55*, 493–505.
- Fabbri, S., Stubbs, K. M., Cusack, R., & Culham, J. C. (2016). Disentangling representations of object and grasp properties in the human brain. *Journal of Neuroscience*, *36*, 7648–7662.
- Fang, F., & He, S. (2005). Cortical responses to invisible objects in the human dorsal and ventral pathways. *Nature Neuroscience*, *8*, 1380–1385.
- Ferrera, V. P., Nealey, T. A., & Maunsell, J. H. (1994). Responses in macaque visual area V4 following inactivation of the parvocellular and magnocellular LGN pathways. *Journal of Neuroscience*, *14*, 2080–2088.
- Freud, E., & Behrmann, M. (2017). The life-span trajectory of visual perception of 3D objects. *Scientific Reports*, *7*, 11034.
- Freud, E., Culham, J. C., Plaut, D. C., & Behrmann, M. (2017). The large-scale organization of shape processing in the ventral and dorsal pathways. *eLife*, *6*, e27576.
- Freud, E., Ganel, T., & Avidan, G. (2015). Impossible expectations: fMRI adaptation in the lateral occipital complex (LOC) is modulated by the statistical regularities of 3D structural information. *Neuroimage*, *122*, 188–194.
- Freud, E., Ganel, T., Shelef, I., Hammer, M. D., Avidan, G., & Behrmann, M. (2017). Three-dimensional representations of objects in dorsal cortex are dissociable from those in ventral cortex. *Cerebral Cortex*, *27*, 422–434.
- Freud, E., Macdonald, S. N., Chen, J., Quinlan, D. J., Goodale, M. A., & Culham, J. C. (2018). Getting a grip on reality: Grasping movements directed to real objects and images rely on dissociable neural representations. *Cortex*, *98*, 34–48.
- Freud, E., Plaut, D. C., & Behrmann, M. (2016). 'What' is happening in the dorsal visual pathway. *Trends in Cognitive Sciences*, *20*, 773–784.
- Freud, E., Rosenthal, G., Ganel, T., & Avidan, G. (2015). Sensitivity to object impossibility in the human visual cortex: Evidence from functional connectivity. *Journal of Cognitive Neuroscience*, *27*, 1029–1043.
- Georgieva, S. S., Peeters, R., Kolster, H., Todd, J. T., & Orban, G. A. (2009). The processing of three-dimensional shape

- from disparity in the human brain. *Journal of Neuroscience*, *29*, 727–742.
- Georgieva, S. S., Todd, J. T., Peeters, R., & Orban, G. A. (2008). The extraction of 3D shape from texture and shading in the human brain. *Cerebral Cortex*, *18*, 2416–2438.
- Goodale, M. A., & Milner, A. D. (1992). Separate visual pathways for perception and action. *Trends in Neurosciences*, *15*, 20–25.
- Han, S., Lungchi, C., & Alais, D. (2016). The temporal frequency tuning of continuous flash suppression reveals peak suppression at very low frequencies. *Scientific Reports*, *6*, 35723.
- Janssen, P., Verhoef, B.-E., & Premereur, E. (2018). Functional interactions between the macaque dorsal and ventral visual pathways during three-dimensional object vision. *Cortex*, *98*, 218–227.
- Jeong, S. K., & Xu, Y. (2016). Behaviorally relevant abstract object identity representation in the human parietal cortex. *Journal of Neuroscience*, *36*, 1607–1619.
- Konen, C. S., & Kastner, S. (2008). Two hierarchically organized neural systems for object information in human visual cortex. *Nature Neuroscience*, *11*, 224–231.
- Kristensen, S., Garcea, F. E., Mahon, B. Z., & Almeida, J. (2016). Temporal frequency tuning reveals interactions between the dorsal and ventral visual streams. *Journal of Cognitive Neuroscience*, *28*, 1295–1302.
- Ludwig, K., & Hesselmann, G. (2015). Weighing the evidence for a dorsal processing bias under continuous flash suppression. *Consciousness and Cognition*, *35*, 251–259.
- Ludwig, K., Kathmann, N., Sterzer, P., & Hesselmann, G. (2015). Investigating category- and shape-selective neural processing in ventral and dorsal visual stream under interocular suppression. *Human Brain Mapping*, *36*, 137–149.
- Lupker, S. J., & Pexman, P. M. (2010). Making things difficult in lexical decision: The impact of pseudohomophones and transposed-letter nonwords on frequency and semantic priming effects. *Journal of Experimental Psychology: Learning, Memory, and Cognition*, *36*, 1267–1289.
- Mahon, B. Z., Kumar, N., & Almeida, J. (2013). Spatial frequency tuning reveals interactions between the dorsal and ventral visual systems. *Journal of Cognitive Neuroscience*, *25*, 862–871.
- Merigan, W. H., & Maunsell, J. H. R. (1993). How parallel are the primate visual pathways? *Annual Review of Neuroscience*, *16*, 369–402.
- Moors, P., Hesselmann, G., Wagemans, J., & van Ee, R. (2017). Continuous flash suppression: Stimulus fractionation rather than integration. *Trends in Cognitive Sciences*, *21*, 719–721.
- Murata, A., Gallese, V., Luppino, G., Kaseda, M., & Sakata, H. (2000). Selectivity for the shape, size, and orientation of objects for grasping in neurons of monkey parietal area AIP. *Journal of Neurophysiology*, *83*, 2580–2601.
- Nassi, J. J., Lyon, D. C., & Callaway, E. M. (2006). The parvocellular LGN provides a robust disynaptic input to the visual motion area MT. *Neuron*, *50*, 319–327.
- Norman, J. F., Bartholomew, A. N., & Burton, C. L. (2008). Aging preserves the ability to perceive 3D object shape from static but not deforming boundary contours. *Acta Psychologica*, *129*, 198–207.
- Orban, G. A. (2011). The extraction of 3D shape in the visual system of human and nonhuman primates. *Annual Review of Neuroscience*, *34*, 361–388.
- Sakuraba, S., Sakai, S., Yamanaka, M., Yokosawa, K., & Hirayama, K. (2012). Does the human dorsal stream really process a category for tools? *Journal of Neuroscience*, *32*, 3949–3953.
- Shikata, E., Hamzei, F., Glauche, V., Knab, R., Dettmers, C., Weiller, C., et al. (2001). Surface orientation discrimination activates caudal and anterior intraparietal sulcus in humans: An event-related fMRI study. *Journal of Neurophysiology*, *85*, 1309–1314.
- Taira, M., Nose, I., Inoue, K., & Tsutsui, K. (2001). Cortical areas related to attention to 3D surface structures based on shading: An fMRI study. *Neuroimage*, *14*, 959–966.
- Tettamanti, M., Conca, F., Falini, A., & Perani, D. (2017). Unaware processing of tools in the neural system for object-directed action representation. *Journal of Neuroscience*, *37*, 10712–10724.
- Theys, T., Pani, P., van Loon, J., Goffin, J., & Janssen, P. (2013). Three-dimensional shape coding in grasping circuits: A comparison between the anterior intraparietal area and ventral premotor area F5a. *Journal of Cognitive Neuroscience*, *25*, 352–364.
- Theys, T., Romero, M. C., van Loon, J., & Janssen, P. (2015). Shape representations in the primate dorsal visual stream. *Frontiers in Computational Neuroscience*, *9*, 43.
- Thomas, C., Kveraga, K., Huberle, E., Karnath, H.-O., & Bar, M. (2012). Enabling global processing in simultanagnosia by psychophysical biasing of visual pathways. *Brain*, *135*, 1578–1585.
- Tsuchiya, N., & Koch, C. (2005). Continuous flash suppression reduces negative afterimages. *Nature Neuroscience*, *8*, 1096–1101.
- Ungerleider, L. G., & Mishkin, M. (1982). Two cortical visual systems. In D. J. Ingle, M. A. Goodale, & R. J. W. Mansfield (Eds.), *Analysis of visual behavior* (pp. 549–586). Cambridge, MA: MIT Press.
- Van Dromme, I. C., Premereur, E., Verhoef, B.-E., Vanduffel, W., & Janssen, P. (2016). Posterior parietal cortex drives inferotemporal activations during three-dimensional object vision. *PLoS Biology*, *14*, e1002445.
- Zachariou, V., Klatzky, R., & Behrmann, M. (2014). Ventral and dorsal visual stream contributions to the perception of object shape and object location. *Journal of Cognitive Neuroscience*, *26*, 189–209.
- Zachariou, V., Nikas, C. V., Safiullah, Z. N., Gotts, S. J., & Ungerleider, L. G. (2017). Spatial mechanisms within the dorsal visual pathway contribute to the configural processing of faces. *Cerebral Cortex*, *27*, 4124–4138.